J Neurophysiol 95: 1843–1852, 2006.
First published November 23, 2005; doi:10.1152/jn.00996.2005.

Lack of the Kir4.1 Channel Subunit Abolishes K^+ Buffering Properties of Astrocytes in the Ventral Respiratory Group: Impact on Extracellular K^+ Regulation

Clemens Neusch,[1] Nestoras Papadopoulos,[2] Michael Müller,[2,4] Iris Maletzki,[1] Stefan M. Winter,[2,4] Johannes Hirrlinger,[3,4] Melanie Handschuh,[1] Mathias Bähr,[1,4] Diethelm W. Richter,[2,4] Frank Kirchhoff,[3,4] and Swen Hülsmann[2,4]

[1]*Departments of Neurology and* [2]*Neuro- and Sensory Physiology, Georg-August-University;* [3]*Department of Neurogenetics, Max-Planck-Institute of Experimental Medicine; and* [4]*Deutsche Forshungsgemeinschaft Research Center for Molecular Physiology of the Brain, Gottingen, Germany*

Submitted 21 September 2005; accepted in final form 15 November 2005

Neusch, Clemens, Nestoras Papadopoulos, Michael Müller, Iris Maletzki, Stefan M. Winter, Johannes Hirrlinger, Melanie Handschuh, Mathias Bähr, Diethelm W. Richter, Frank Kirchhoff, and Swen Hülsmann. Lack of the Kir4. 1 channel subunit abolishes K^+ buffering properties of astrocytes in the ventral respiratory group: impact on extracellular K^+ regulation. *J Neurophysiol* 95: 1843–1852, 2006. First published November 23, 2005; doi:10.1152/jn.00996.2005. Ongoing rhythmic neuronal activity in the ventral respiratory group (VRG) of the brain stem results in periodic changes of extracellular K^+. To estimate the involvement of the weakly inwardly rectifying K^+ channel Kir4.1 (KCNJ10) in extracellular K^+ clearance, we examined its functional expression in astrocytes of the respiratory network. Kir4.1 was expressed in astroglial cells of the VRG, predominantly in fine astrocytic processes surrounding capillaries and in close proximity to VRG neurons. Kir4.1 expression was up-regulated during early postnatal development. The physiological role of astrocytic Kir4.1 was studied using mice with a null mutation in the Kir4.1 channel gene that were interbred with transgenic mice expressing the enhanced green fluorescent protein in their astrocytes. The membrane potential was depolarized in astrocytes of Kir4.1$^{-/-}$ mice, and Ba^{2+}-sensitive inward K^+ currents were diminished. Brain slices from Kir4.1$^{-/-}$ mice, containing the pre-Bötzinger complex, which generates a respiratory rhythm, did not show any obvious differences in rhythmic bursting activity compared with wild-type controls, indicating that the lack of Kir4.1 channels alone does not impair respiratory network activity. Extracellular K^+ measurements revealed that Kir4.1 channels contribute to extracellular K^+ regulation. Kir4.1 channels reduce baseline K^+ levels, and they compensate for the K^+ undershoot. Our data indicate that Kir4.1 channels *1*) are expressed in perineuronal processes of astrocytes, *2*) constitute the major part of the astrocytic Kir conductance, and *3*) contribute to regulation of extracellular K^+ in the respiratory network.

INTRODUCTION

In the mammalian brain, astrocytes provide not only metabolic substrates to neurons, but they also have an important influence on synaptic transmission (Gomeza et al. 2003; Haydon 2001; Hülsmann et al. 2000; Magistretti et al. 1999). The latter function strongly depends on the glial capacity to regulate the extracellular ionic environment, particularly the interstitial K^+ concentration. This "spatial buffering" depends on the expression of various glial K^+ channels including inwardly rectifying K^+ channels (Kir). During ongoing neuronal activity, these channels mediate the influx of K^+ into astrocytes (Arcangeli et al. 1993; Gardner-Medwin et al. 1981; Kofuji et al. 2000, 2002; Neusch et al. 2001; Newman 1986, 1987, 1993; Newman et al. 1984; Richter et al. 1978; Rozengurt et al. 2003). Furthermore, Kir channels regulate the activity of glial cells themselves by setting the resting membrane potential (RMP), controlling transmembrane transport of other signaling molecules (Neusch et al. 2001) and regulating cell differentiation (Arcangeli et al. 1993, 1995; Kusaka et al. 1999; Lepple-Wienhues et al. 1996)

Within the lower brain stem, the respiratory rhythm is generated and adjusted by a neuronal network located within the ventral respiratory group (VRG) (Richter and Spyer 2001), including the pre-Bötzinger complex that is involved in respiratory rhythm generation (Ramirez et al. 1998; Smith et al. 1991). In this kernel, the majority of astrocytes show a high potassium conductance, which indicates that they make an important contribution to local potassium buffering (Graβ et al. 2004). Thus it is not surprising that the overall changes in extracellular K^+ remain rather small during periodic neuronal discharges (Brockhaus et al. 1993; Richter et al. 1978).

One possible candidate for *trans*-membranous K^+ fluxes in astrocytes of the respiratory network is the weakly inwardly rectifying K^+ channel Kir4.1 (KCNJ10). The Kir4.1 channel subunit is expressed predominantly in glial cells (Neusch et al. 2001; Takumi et al. 1995) and to a lesser degree in neurons (Bredt et al. 1995; Jiang et al. 2001; Li et al. 2001). In the brain stem, mRNA for Kir4.1 was detected in respiratory regions including the VRG and the pre-Bötzinger complex (Wu et al. 2004). Therefore we used immunohistochemical methods to assess the expression of the Kir4.1 subunit in astrocytes of the VRG, and in electrophysiological experiments, we studied its functional relevance for the stabilization of the respiratory network activity. To address the role of Kir4.1 in ion homeostasis, we took advantage of a mouse line with a specific ablation of the *Kir4.1* gene (Kofuji et al. 2000; Marcus et al. 2002; Neusch et al. 2001; Rozengurt et al. 2003). To identify

Address for reprint requests and other correspondence: S. Hülsmann, Dept. of Neuro- and Sensory Physiology, Georg-August-Univ. Göttingen, Humboldtallee 23, 37073 Göttingen, Germany (E-mail: shuelsm2@uni-goettingen.de).

The costs of publication of this article were defrayed in part by the payment of page charges. The article must therefore be hereby marked "*advertisement*" in accordance with 18 U.S.C. Section 1734 solely to indicate this fact.

astrocytes in the pre-Bötzinger region we generated double transgenic mice by interbreeding Kir4.1 heterozygous animals with transgenic mice expressing the enhanced green fluorescent protein (EGFP) under the control of the astrocyte-specific human glia fibrillary acidic protein (hGFAP) promoter [TgN-(hGFAP-EGFP); Nolte et al. 2001].

METHODS

Interbreeding of transgenic mice expressing EGFP under the GFAP promoter and mice with Kir4.1 subunit gene ablation

Generation of Kir4.1$^{-/-}$ mice and transgenic mice expressing the fluorescent protein EGFP under the human GFAP promoter [TgN (hGFAP-EGFP)] was described previously (Kofuji et al. 2000; Nolte et al. 2001). Both mouse lines were interbred to generate double transgenic mice. Mice from the F2–F4 generations were used in this study. Genotyping was performed as previously described (Kofuji et al. 2000; Nolte et al. 2001).

Histology, immunohistochemistry, and immunofluorescence

Animals >10 days were anesthetized and perfused by transcardial injection with PBS followed by 4% paraformaldehyde (PFA) in PBS. The brain stem and cerebellum were removed and postfixed in 4% PFA overnight. Animals from postnatal days 5–9 (P5–P9) were anesthetized and rapidly decapitated. Brains were immersion-fixed in 10% PFA overnight, followed by dehydration in 70% ethanol for 48 h. The brain stem and cerebellum were embedded in paraffin and sectioned at 10–12 μm.

For immunohistochemistry, paraffin sections were dewaxed in xylene and dehydrated in ethanol, rehydrated, and incubated for 10 min at 55°C followed by boiling at 95°C in an antigen demasking solution (Vector Laboratories, Burlingame, CA) for another 10 min.

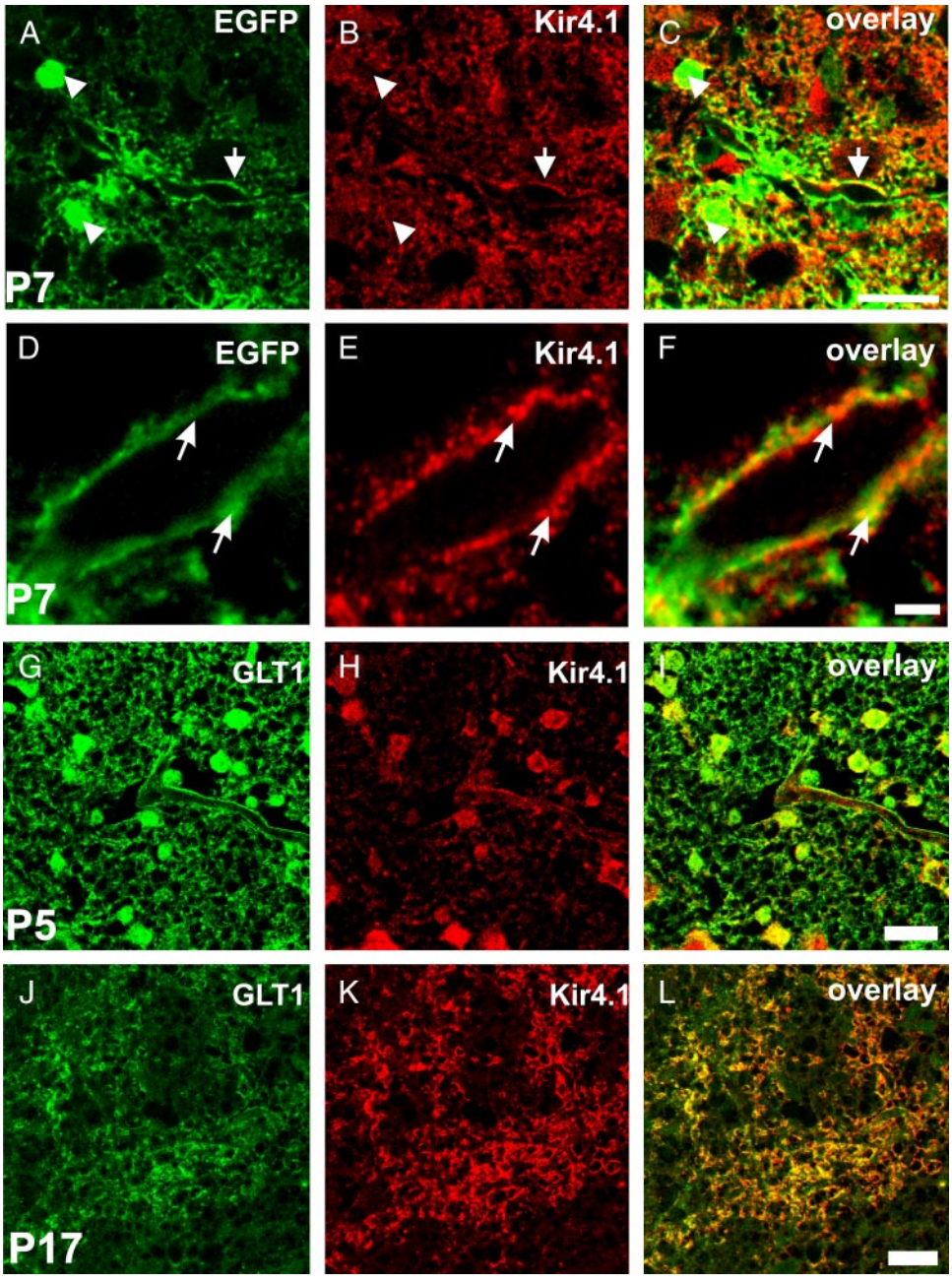

FIG. 1. Expression of the Kir4.1 channel subunit is shown in the ventral respiratory group. *A*: enhanced green fluorescent protein (EGFP)-fluorescent astrocytes. *B*: Kir4.1 is abundantly expressed in the astroglial network and on glial endfeet surrounding small capillaries (arrows) but only weakly labels astroglial cell bodies (arrowheads). *C*: overlay of *A* and *B*. Obtained at higher magnification and show clustered expression of Kir4.1 on astroglial endfeet (*E*), which embrace a capillary (*D*). *F*: overlay of *E* and *D*. *G–I*: glutamate transporter I (GLT1) immunolabeling of astrocytes at P5 where expression occurred predominantly in astroglial cell bodies (*G*). *H*: Kir4.1 channel expression on astrocytes co-localized with GLT1 expression (*I* is an overlay of *G* and *H*). *J–L*: developmental changes of GLT1 and Kir4.1 protein expression. *J*: obtained at P17 when GLT1 expression was predominantly in astroglial processes. *K*: Kir4.1 antibody labels astroglial processes extensively and labels astroglial cell bodies only weakly. *L*: overlay of *J* and *K* and documents that GLT1 and Kir4.1 co-localize on astroglial membranes. Scale bar, 20 (*A–C* and *G–L*) and 2 μm (*D–F*).

After blocking for 20 min in 0.2% Triton X-100 and 10% normal goat serum (NGS) in PBS, sections were treated in another blocking step with 5% dry milk (30 min). The samples were washed and incubated with the primary antibody in 1% NGS at 4°C overnight. Samples were incubated with a fluorescent Cy3- (goat, 1:1,000) or Cy5-conjugated (goat, 1:500) secondary antibody (Jackson Immunoresearch, West Grove, PA) for 1 h at room temperature. The following primary antibody concentrations were used: Kir4.1 (rabbit, 1:100; Alomone) and glutamate transporter I (GLT1; guinea pig, 1:100; Chemicon). The Nissl staining was done according to the manufacturer's protocol (Molecular Probes). Confocal images of 10- 12-μm brain stem sections were obtained on a confocal laser-scanning microscope (LSM 510 Meta, Zeiss Oberkochen) equipped with two HeNe lasers (546- and 633-nm wavelength) and one argon laser (488 nm). EGFP was excited at 488 nm, and fluorescence was detected through a 500- to 550-nm band-pass filter (Cy3: 543-nm/565- to 615-nm band-pass filter; Cy5; 633-nm/650-nm long-pass filter).

Electrophysiological recording of astrocytes in brain stem slices

The Kir $4.1^{-/-}$ knock-out mice usually died in the first 2 postnatal weeks (Neusch et al. 2001). Thus mice from P6 to P11 were used for electrophysiological studies. Mice were decapitated, and the brain stem was removed and placed in cooled artificial cerebrospinal fluid (ACSF) equilibrated with oxygen and carbon dioxide (95% O_2-5% CO_2). Transverse slices (200–300 μm) from the caudal medulla were cut with a vibroslicer (Campden Instruments, Loughborough, UK) and stored in ACSF at room temperature (21–24°C) for ≥30 min before experiments were started. Slices were subsequently transferred to a recording chamber and kept submerged by nylon fibers. The chamber was continuously superfused with ACSF (room temperature; 21–24°C) at a flow rate of 10–20 ml/min. The composition of the ACSF (Hülsmann et al. 2000) was (in mM) 118 NaCl, 3 KCl, 1.5 $CaCl_2$, 1 $MgCl_2$, 1 NaH_2PO_4, 25 $NaHCO_3$, and 30 D-glucose (330 mosmol/l; pH 7.4). Thick slice preparations of neonatal animals work better using high extracellular glucose because of their high capacity to use anaerobic (glycolytic) metabolism for ATP production (Ballanyi 2004). To analyze Kir currents, 50 mM NaCl of the external solution was replaced by 50 mM KCl. To block inwardly rectifying K^+ currents, 1 mM Ba^{2+} was added to this solution.

EGFP fluorescence was excited at 467 nm with a computer-controlled monochromator (dichroic mirror, 495 nm; Polychrome II, TILL Photonics, Gräfelling, Germany). Only astrocytes that displayed a clear bright green fluorescence were studied; astrocytes with weak fluorescence were not used in this study because they are likely to represent a different cell population (Graβ et al. 2004; Matthias et al. 2003).

Patch electrodes were pulled from borosilicate glass capillaries (Biomedical Instruments, Zöllnitz, Germany) on a horizontal pipette-puller (Zeitz-Instrumente, Munich, Germany) filled with (in mM) 125 KCl, 1 $CaCl_2$, 10 EGTA, 2 $MgCl_2$, 4 Na_2ATP, 10 HEPES (pH was adjusted to 7.2 with KOH.). Patch electrode resistances were 2–6 MΩ. Astrocytes were clamped to −80 mV and exposed to different voltage step protocols as indicated below. Whole cell currents were measured with a Multiclamp 700A amplifier (Axon Instruments, Foster City, CA), filtered at 2 kHz, digitized at 10 KHz, and stored on a computer using the pCLAMP 9.2 software (Axon Instruments).

Rhythmic slice preparation

A single 650- to 750-μm-thick cut was made from the medulla to obtain one slice containing the functionally intact pre-Bötzinger complex (PBC) and the projections from the PBC to the hypoglossal nucleus and the hypoglossal (XII) rootlets (Ramirez et al. 1996, 1998; Smith et al. 1991). The slice was transferred to a recording chamber superfused with an ACSF solution that was saturated with 95% O_2-5% CO_2 at 30°C. Extracellular K^+ was elevated to 8 mM to maintain respiratory network activity. Rhythmic mass activity from the pre-Bötzinger complex and activity from nerve rootlets of the

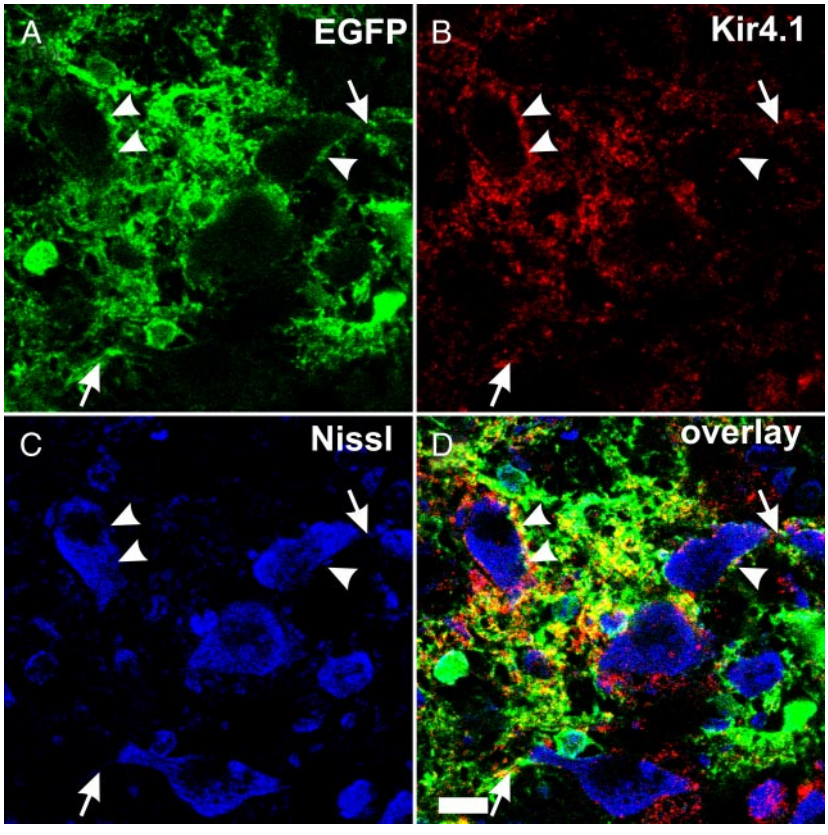

FIG. 2. Kir4.1 is expressed in astroglial processes embracing neuronal structures (*A–D*). *C*: confocal image showing Nissl-positive neurons in the ventral respiratory group (VRG). Kir4.1 staining was frequently detected in close proximity to neuronal somata (arrowheads) and dendrites (arrows; *B*), but localized to processes of EGFP-positive astrocytes (*A*) in most of the observed areas. *D*: overlay of *A–C*. Scale bar, 10 μm.

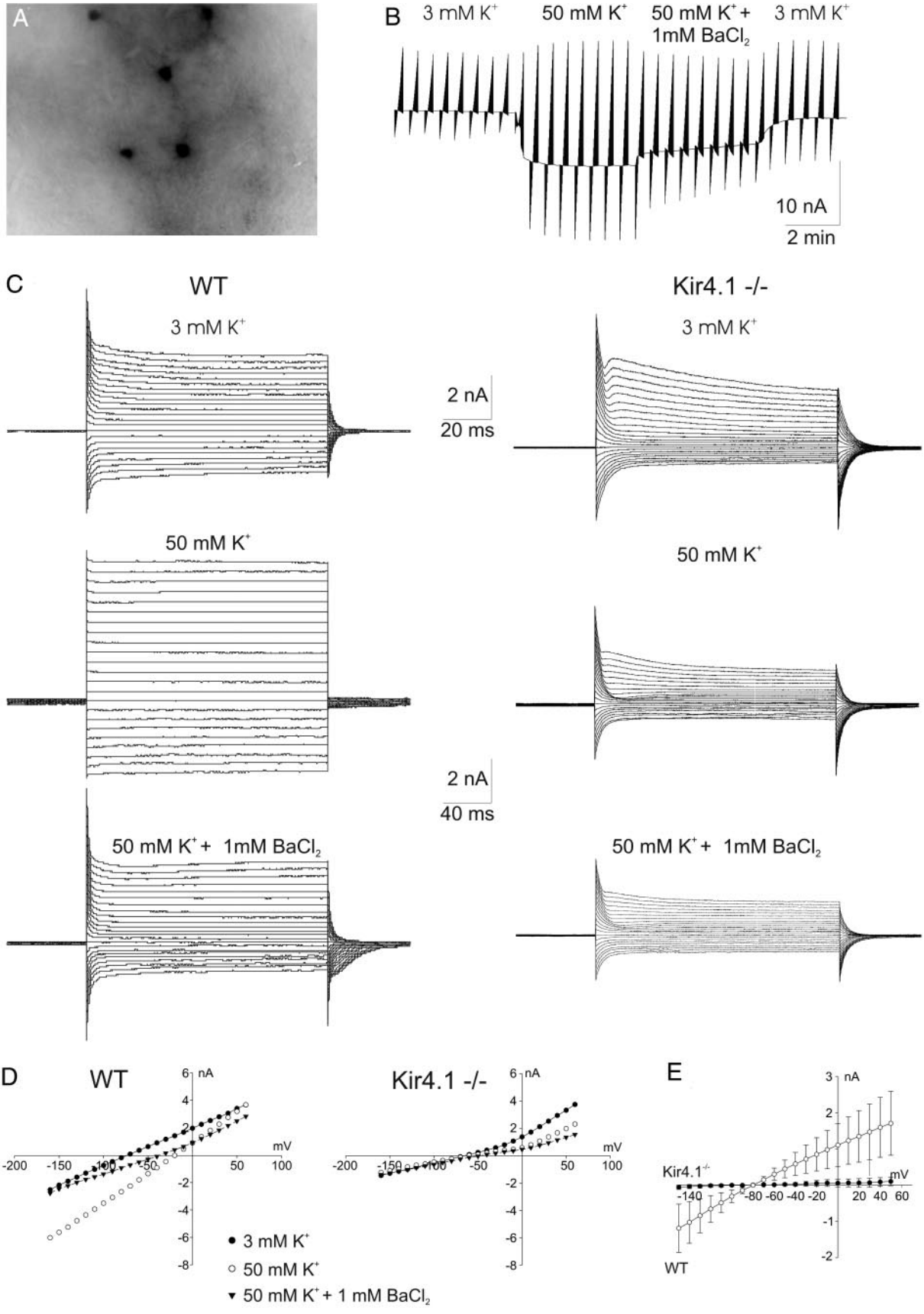

TABLE 1. *Electrophysiological properties of WT, Kir4.1$^{+/-}$, and Kir4.1$^{-/-}$ astrocytes in the VRG*

	WT	Kir4.1$^{+/-}$	Kir4.1$^{-/-}$
$I_{(-150)}$[nA]	−2.0 ± 0.7 (17)	−1.9 ± 0.9 (31)	−1.5 ± 0.9* (39)
Change of $I_{(-150)}$ in 50 mM KCl, nA	−1.2 ± 2.1 (15)	−0.6 ± 0.9 (31)	−0.1 ± 0.5* (24)
Ba^{2+}-sensitive $I_{(-150)}$ current, nA in 50 mM K^+	−1.2 ± 1.8 (7)	−0.5 ± 0.8 (22)	−0.1 ± 0.1* (7)
RMP, mV	−72.2 ± 10.5 (17)	−71.4 ± 17.7 (31)	−49.2 ± 10.5* (39)
R_{in}, MΩ	38.0 ± 12.6 (17)	44.2 ± 20.1 (31)	67.3 ± 51.1* (39)

Values are mean ± SD. Brain slice recordings of astrocytes in the VRG. Number in parentheses indicates the number of whole cell voltage-clamp experiments. Mice used for the experiments were from P6-P11. *Significant values ($P < 0.05$), compared with WT experiments. VRG, ventral respiratary group; WT, wild type.

hypoglossal nucleus was recorded with extracellular glass capillary microelectrodes. The frequency of the rhythmic burst activity, which is in phase with the hypoglossal activity (Johnson et al. 2001), was used as the parameter for the central respiratory rhythm (Smith et al. 1991). Recordings were amplified 5,000–10,000 times, band-pass filtered (0.25–1.5 kHz), rectified, and integrated (Paynter filter with a time constant of 50–100 ms). Extracellular field potentials and the integrals were digitized (Digidata 1320, Axon Instruments) at 5 KHz and stored on a computer using pCLAMP 9.2 (Axon Instruments). Burst frequency was calculated from the interburst interval of 3-min segments.

Extracellular K^+ measurements in brain stem slices

Measurements of extracellular K^+ ($[K^+]_o$) were made in an interface recording chamber of the Oslo style (Müller and Somjen 2000) to reduce wash out of extracellular K^+. Slices were kept at a temperature of 32°C and were perfused with ACSF (1.5 ml/min) aerated continuously with 95% O_2-5% CO_2 (400 ml/min). Changes of $[K^+]_o$ were measured using double-barreled K^+-sensitive microelectrodes (Müller and Somjen 2000). They were pulled from theta type capillaries (Clark GCT 200–10, Harvard Apparatus) on a horizontal puller (P97, Flaming Brown, Sutter Instruments). The ion-sensitive barrel was silanized by 105-min exposure to hexamethyldisilazane vapors (98%, Fluka; vaporized at 40°C) and subsequently baked at 220°C for 2 h. Silanization of the reference barrel was prevented by perfusing it with nitrogen (1.5 bar). The tip of the K^+-sensitive barrel was filled with the valinomycin based K^+ ion neutral carrier (potassium ionophore I–cocktail A, Fluka 60031) and backfilled with 150 mM KCl + 10 mM HEPES, pH 7.4. The reference barrel contained 150 mM NaCl + 10 mM HEPES, pH 7.4. Electrode resistances of the reference and ion-sensitive barrel were 10–20 and 170–250 MΩ, respectively. K^+-sensitive electrodes were calibrated before and after each experiment by detecting the response of each electrode to standard solutions (0, 1, 2, 5, 10, 20, 50, and 100 mM K^+). To maintain constant ionic strength similar to that in interstitial fluid, Na^+ in the calibration solutions was replaced by K^+ and vice versa (reciprocal calibration method). Ion-sensitive electrode signals were amplified with a differential electrometer (FD 223, World Precision Instruments) and digitized by a TL-1/Axotape acquisition system (Axon Instruments) at sampling rates of 1 kHz. $[K^+]_o$ was calculated directly from the electrode responses using the slope of the calibration curve.

To measure rhythmic changes in the $[K^+]_o$ under comparable conditions, we recorded stimulation-induced changes of $[K^+]_o$. Stimulating electrodes made from bare stainless steel wire (50 μm diam, AM Systems) were positioned in the midline of the slice, while the K^+ sensitive electrode was placed in the VRG. Changes in $[K^+]_o$ resulting from three consecutive bursts (1-s duration) of 15-μA constant current pulses (0.1-ms pulse width at 100 Hz) applied at a frequency of 1 min^{-1} were analyzed.

Data processing

Data were analyzed with SigmaPlot/SigmaStat (Systat Software, Point Richmond, CA). The unpaired *t*-test and the Mann-Whitney rank sum test were used to determine the significance of changes when comparing values obtained from Kir4.1$^{-/-}$ to WT mice. Results were expressed as mean ± SD, and differences were considered significant if $P < 0.05$.

RESULTS

Kir4.1 is expressed in VRG astrocytes and is targeted to astroglial processes during postnatal development

Kir 4.1 protein expression in astrocytes of the VRG was shown using two different markers for astrocytes. Kir 4.1 immunoreactivity overlapped the transgenic expression of EGFP in astrocytic somata and their processes (Fig. 1, *A–C*), including astroglial endfeet structures embracing the microvasculature (Fig. 1, *D–F*). This observation was verified when astrocytes were identified on the basis of the glial GLT1 (Fig. 1, *G–L*). During developmental maturation of the network, Kir4.1 channel distribution changed. In the first postnatal week (P5), Kir4.1 immunolabeling in the VRG was found predominantly on cell bodies of astrocytes (Fig. 1, *G–I*). From the second postnatal week on, Kir4.1 immunostaining on cell bodies decreased, and the expression of Kir4.1 shifted to astrocytic processes (Fig. 1, *J–L*).

The Kir4.1 antibody also labeled to some extent neurons in the VRG (data not shown). However, the most intense Kir4.1 staining was co-localized with EGFP-labeled astrocytic structures, often in close proximity to neuronal cell bodies (Fig. 2, *A–D*, arrowheads) and dendrites (arrows), thereby providing immunohistochemical proof of its glial location. The close proximity to neuronal structure supports a putative role in K^+ regulation associated with neuronal activity.

FIG. 3. Electrophysiological properties of wild-type (WT) and Kir4.1$^{-/-}$ astrocytes in the VRG of brain stem slices. *A*: inverted CCD camera image showing EGFP-positive astrocytes in the VRG of a WT mouse. *B*: continuous recording from a WT astrocyte. Astrocyte was clamped at −80 mV and repetitively (4 min^{-1}) stepped to potentials ranging from −160 to +60 mV in 10 mV increments. Corresponding currents were taken to determine *I-V* curves. Extracellular K^+ was increased from 3 mM K^+ to 50 mM followed by additional application of 1 mM $BaCl_2$. *C*: exemplary whole cell currents derived from the step protocol recorded for WT and Kir4.1$^{-/-}$ astrocyte in the presence of 3 mM K^+, 50 mM K^+, and 50 mM K^+ plus 1 mM Ba^{2+}. *D*: *I-V* curves determined from steady-state level of whole cell currents shown in *C* for WT and Kir4.1$^{-/-}$. *E*: averaged *I-V* curves resulting from subtracting currents in 50 mM K^+ from corresponding currents taken during Ba^{2+} (1 mM) blockade (mean ± SE; WT, $n = 7$; Kir4.1$^{-/-}$, $n = 7$).

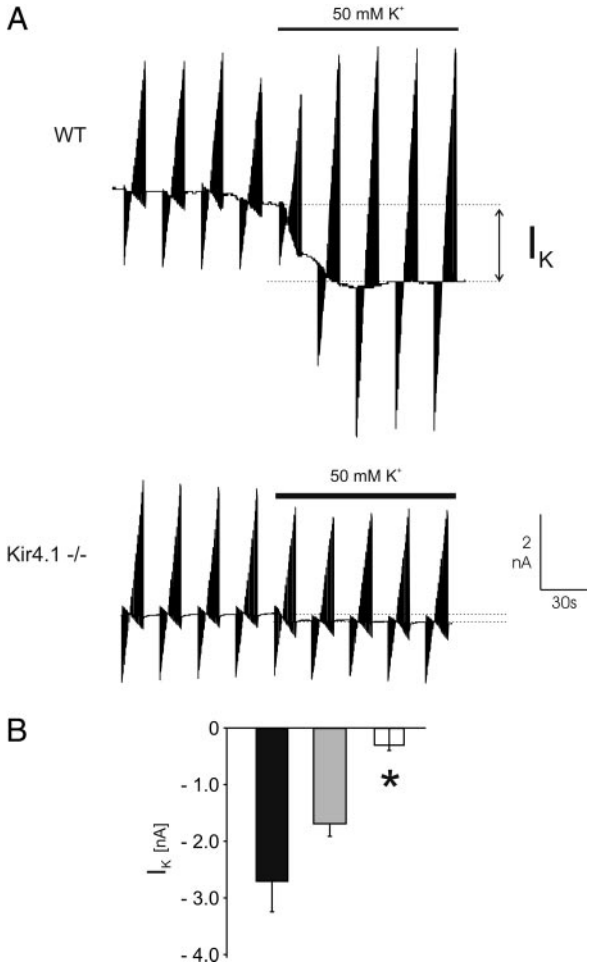

FIG. 4. Astrocytes of Kir4.1$^{-/-}$ mice have reduced K^+ uptake capabilities. *A*: continuous voltage-clamp recordings (V_{hold} −80 mV) show that application of 50 mM K^+ elicited a strong inward current (I_K) in WT but not in Kir4.1$^{-/-}$ astrocytes. *B*: statistical summary of the I_K in WT (filled bar), Kir4.1$^{\pm}$ (gray bar), and Kir4.1$^{-/-}$ (open bar) astrocytes. Data are given as mean ± SD for WT (n = 15), Kir4.1$^{+/-}$ (n = 31), and Kir4.1$^{-/-}$ (n = 24) astrocytes (*significance: $P < 0.05$).

Brain stem astrocytes from Kir4.1$^{-/-}$ mice are depolarized

To confirm our immunohistochemical data and to understand the functional impact of Kir4.1 channels on astrocytic membrane properties, we performed whole cell voltage-clamp recordings from WT and Kir4.1$^{-/-}$ astrocytes in medullary slices (Fig. 3*A*). WT and Kir4.1$^{-/-}$ astrocytes exhibited different electrophysiological properties: the RMP of Kir4.1$^{-/-}$ astrocytes (−49.2 ± 10.5 mV, n = 39) was depolarized ($P <$ 0.001) compared with WT astrocytes (−72.2 ± 10.5 mV, n = 17, $P < 0.001$), which is consistent with the finding that astrocytic input resistance was higher (67.3 ± 51.1 MΩ; n = 39) in Kir4.1$^{-/-}$ mice than in WT astrocytes (38.0 ± 12.6 MΩ, n = 17; Table 1; $P = 0.023$). The RMP in astrocytes from heterozygotes (Kir4.1$^{+/-}$) was −71.4 ± 17.7 mV (not significant, n = 31); the input resistance was 44.2 ± 20.1 MΩ (n = 31).

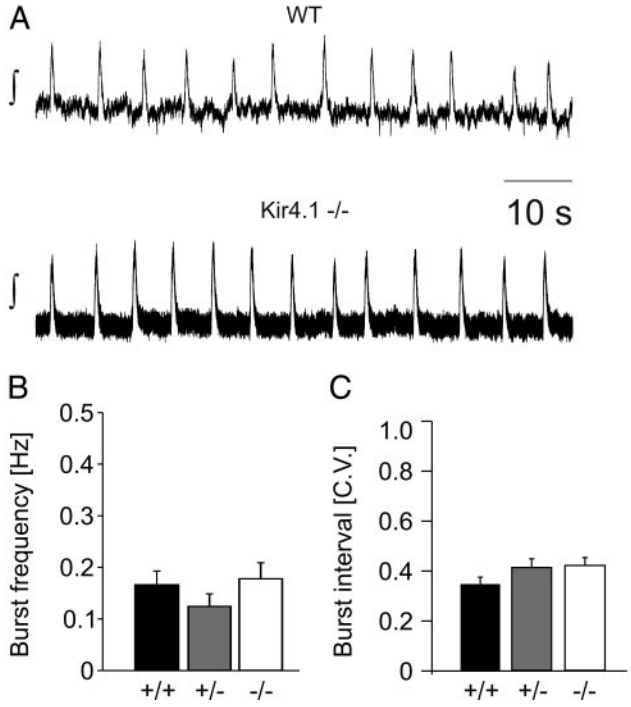

FIG. 5. Genetic deletion of the Kir4.1 channel subunit does not impair rhythm generation in the pre-Bötzinger complex. *A*: integrated respiratory burst activity recorded from rhythmic slices isolated from a WT and Kir4.1$^{-/-}$ mouse at P9. *B*: respiratory burst frequencies and CV (*C*) of the interburst interval determined from brain stem slices of WT (n = 10), Kir4.1$^{\pm}$ (n = 16), and Kir4.1$^{-/-}$ mice (n = 14, P6–P11) do not differ significantly.

Astrocytes were voltage clamped to −80 mV and the current-voltage (*I/V*) relationship was measured in the range of −160 to +60 mV (10-mV increments; Fig. 3, *C*). In ACSF, WT astrocytes showed an almost linear *I/V* curve, whereas astrocytes from Kir4.1$^{-/-}$ mice showed outward rectification (Fig. 3*D*). In 50 mM K^+ containing ACSF, the *I/V* curve was steeper in WT than in Kir4.1$^{-/-}$ astrocytes. Inwardly rectifying K^+ channel currents were isolated by subtracting currents in 50 mM K^+ from corresponding currents taken during Ba^{2+} (1 mM) blockade (Fig. 3, *C* and *D*). The resulting *I/V* curve revealed that inwardly rectifying K^+ currents were almost absent in Kir4.1$^{-/-}$astrocytes (Fig. 3*E*).

To compare Kir currents directly between WT and Kir4.1$^{-/-}$ astrocytes, we quantified the inward current evoked by a voltage step from −80 to −150 mV ($I_{(-150)}$). In control ACSF, this current was smaller in Kir4.1$^{-/-}$ than in WT astrocytes (Table 1). In 50 mM K^+ ACSF, the $I_{(-150)}$ increased by −1.2 ± 2.1 nA in WT (n = 15) and by −0.6 ± 0.9 nA in Kir4.1$^{+/-}$ (not significant, n = 31), but inward rectification was virtually absent in Kir4.1$^{-/-}$ astrocytes ($\Delta I_{(-150)}$ = −0.1 ± 0.5 nA; $P < 0.05$ compared with WT; n = 24).

The barium-sensitive Kir current was calculated by subtracting the $I_{(-150)}$ measured before and after application of 1 mM $BaCl_2$. It was virtually absent in Kir4.1$^{-/-}$ astrocytes (−0.1 ± 0.1 nA; n = 7; Table 1) compared with WT (−1.2 ± 1.8 nA,

FIG. 6. *A*: stimulation-induced $[K^+]_o$ changes recorded in the VRG in WT and Kir4.1$^{-/-}$ mice in artificial cerebrospinal fluid (ACSF) and after application of 1 mM $BaCl_2$. *B*: averaged values of the stimulus-induced changes of K^+ ($\Delta[K^+]_o$) from WT (n = 6) and Kir4.1$^{-/-}$ slices (n = 5). *C*: Ba^{2+} induced increase of the $[K^+]_o$ baseline. *D*: time-course of $[K^+]_o$ recovery after stimulation. *E*: $[K^+]_o$ baseline undershoot after 3 consecutive stimulus-induced K^+ transients as indicated in *A* (mean ± SD; *significance: $P < 0.05$).

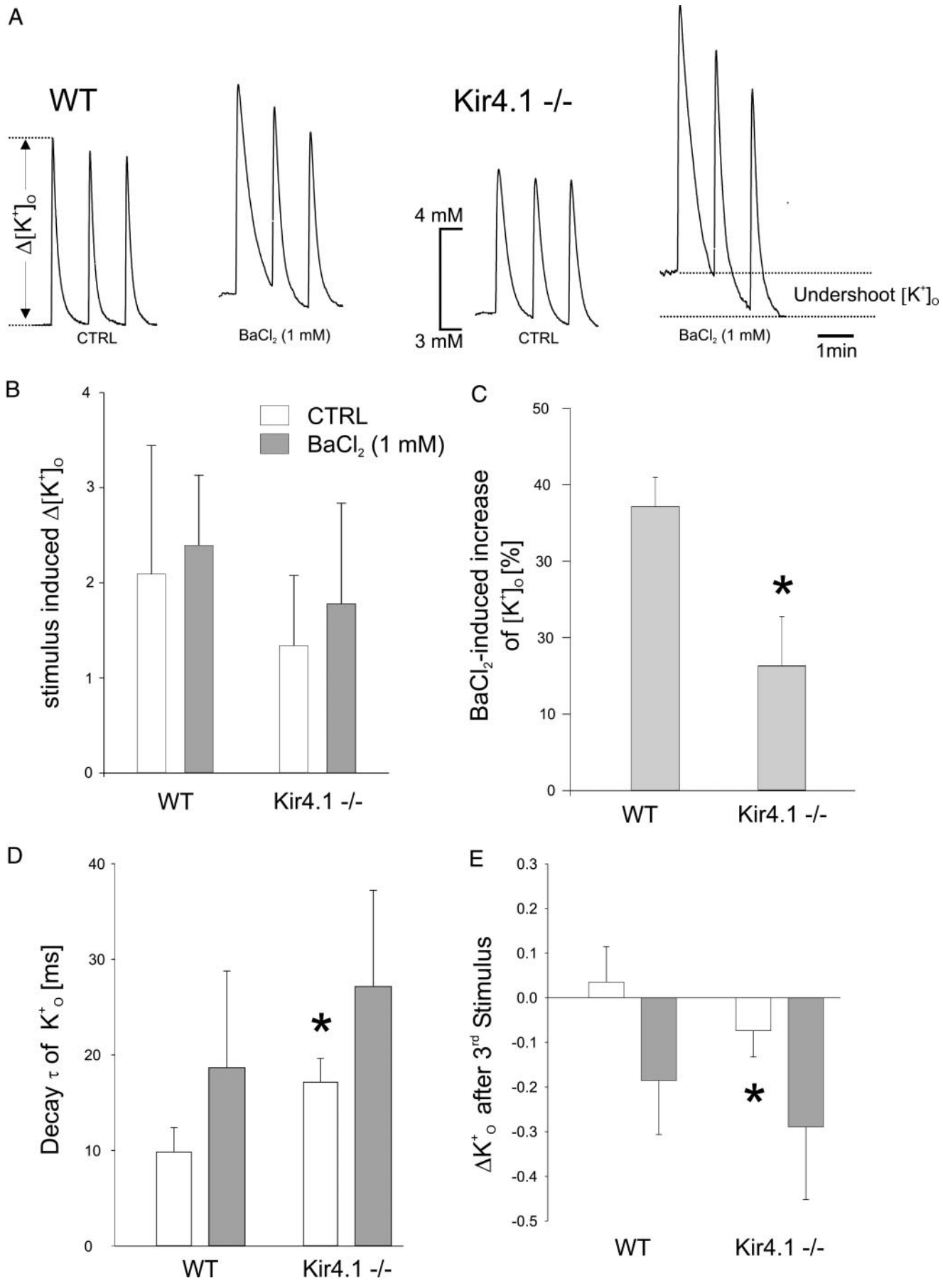

$P < 0.05$; $n = 7$) and Kir4.1$^{+/-}$ astrocytes (-0.5 ± 0.8 nA; $n = 22$).

K^+ uptake properties are disturbed in astrocytes from Kir4.1$^{-/-}$ mice

In WT animals clamped to -80 mV, application of 50 mM K^+ elicited a large inward current of -2.7 ± 0.5 nA ($n = 15$, I_K, Fig. 4, *A* and *B*). This inward current (I_K) was much smaller in Kir4.1$^{-/-}$ astrocytes (-0.3 ± 0.1 nA; $P < 0.001$, $n = 24$), and it had an intermediate magnitude in Kir4.1$^{+/-}$ mice (-1.7 ± 0.2 nA; not significant, $n = 31$; Fig. 4*B*). This indicates that the capacity for K^+ influx at physiological membrane potentials is almost abolished in Kir4.1$^{-/-}$ astrocytes.

Network activity is normal in rhythmic slices of Kir4.1$^{-/-}$

The neuronal network activity of rhythmic brain stem slices was compared in WT and Kir4.1$^{-/-}$ littermates. Slices from WT animals and Kir4.1$^{+/-}$ mice (P6–P11) generated rhythmic burst discharges at frequencies of 0.17 ± 0.03 ($n = 10$) and 0.12 ± 0.02 Hz ($n = 16$, not significant), respectively. The burst frequency was similar in slices from Kir4.1$^{-/-}$ mice (0.18 ± 0.03 Hz, $n = 14$, not significant; Figure 5*B*). The variability of the interburst intervals (CV) did not differ in the three groups (WT: 0.34 ± 0.03; Kir4.1$^{\pm}$ mice: 0.41 ± 0.04, in Kir4.1$^{-/-}$ mice: 0.42 ± 0.03; Fig. 5*C*, not significant).

Regulation of activity-induced extracellular K^+ transients remains functionally intact in Kir 4.1$^{-/-}$ mice

Our data indicate that lack of the Kir4.1 channel subunit does not impair normal respiratory network activity. To directly analyze the function of Kir4.1 channels in the regulation of extracellular K^+, we monitored extracellular K^+ levels under control conditions and after application of 1 mM $BaCl_2$ using ion-selective microelectrodes (Fig. 6*A*).

In normal ACSF, the stimulus-induced K^+ increase was similar in WT (2.1 ± 1.4 mM, $n = 6$) and Kir4.1$^{-/-}$ slices (1.3 ± 0.7 mM, $n = 5$; Fig. 6*B*). The peak levels of the stimulus-induced K^+ transients measured in the presence of 1 mM $BaCl_2$ did not differ in WT (2.4 ± 0.7 mM; $n = 6$) and Kir4.1$^{-/-}$ mice (1.8 ± 1.1 mM; $n = 5$; Fig. 6*B*). A difference was observed, however, for barium-induced changes in $[K^+]_o$ baseline levels. Baseline $[K^+]_o$ rose by $37.2 \pm 3.8\%$ in WT mice but only by $16.3 \pm 6.4\%$ ($P < 0.001$, Fig. 6*C*) in Kir4.1$^{-/-}$ mice.

Another clear difference between WT and Kir 4.1$^{-/-}$ slices was the recovery of $[K^+]_o$ after the first of three consecutive stimuli. In WT slices $[K^+]_o$ decayed with a time constant of 9.8 ± 2.6 s ($n = 6$), while recovery was much slower in Kir4.1$^{-/-}$ mice (17.1 ± 2.5 s; $n = 5$; $P < 0.001$, Fig. 6*D*). $BaCl_2$ application almost doubled the $[K^+]_o$ decay time constant in WT slices (18.7 ± 10.1 s) while the already slower recovery in Kir4.1$^{-/-}$ mice tended to be delayed even more (27.2 ± 10.0 s; not significant; Fig. 6*D*).

Furthermore, after three consecutive stimuli, $[K^+]_o$ in WT slices recovered to a slightly elevated baseline $[K^+]_o$ ($+0.04 \pm 0.09$ mM; Fig. 6*E*), whereas Kir4.1$^{-/-}$ slices showed a clear undershoot of $[K^+]_o$ baseline (-0.07 ± 0.06 mM; $P < 0.05$). A comparable undershoot was obtained in WT slices in the presence 1 mM $BaCl_2$ (-0.18 ± 0.13 mM, $P < 0.01$). In Kir4.1$^{-/-}$ mice, barium application further increased the $[K^+]_o$ undershoot (-0.29 ± 0.16 mM; $P < 0.05$; Fig. 6*E*).

DISCUSSION

Buffering of extracellular K^+ is one of the basic functions of astrocytes. In this study, we show that one candidate for K^+ buffering, the Kir4.1 channel subunit, is up-regulated in the VRG during postnatal maturation. Remarkably, this up-regulation coincides with the developmental stabilization of respiratory network activity (Viemari et al. 2003). The electrophysiological characterization of Kir4.1$^{-/-}$ astrocytes showed that Kir4.1 mediates most of the Kir current in astrocytes, and therefore Kir4.1 is a primary molecular substrate of astroglial K^+ transport. However, overall network activity in the isolated network of pre-Bötzinger complex was not impaired in Kir4.1$^{-/-}$ mice, suggesting that astroglial Kir4.1 channels are not the sole channel responsible for extracellular potassium regulation, but one player among many in the coordinated process of extracellular K^+ regulation.

Our immunohistochemical data indicate that *1*) Kir4.1 expression occurs in astroglial processes in close proximity to neuronal somata and dendrites, and *2*) Kir4.1 channels cluster around small blood vessels and capillaries. This "polarized" distribution of Kir4.1 channels supports the hypothesis that Kir channels mediate uptake of K^+ released by neurons and release potassium to capillaries and small vessels (Higashi et al. 2001; Poopalasundaram et al. 2000; Takumi et al. 1995). Therefore, Kir4.1 localization is well matched to its putative role in regulation of $[K^+]_o$.

Kir currents are reduced in Kir4.1$^{-/-}$ astrocytes

Loss of the Kir4.1 subunit resulted in significant physiological changes in astrocytes: the resting membrane potential was markedly depolarized, the input resistance was increased, and Kir currents were decreased. These observations are consistent with and extend previous reports based on studies of retinal Müller cells (Kofuji et al. 2000) and spinal oligodendrocytes (Neusch et al. 2001), which showed that the lack of Kir4.1 depolarized the resting membrane potential of glial cells.

Fluctuations in $[K^+]_o$ remained well controlled in close proximity to highly active respiratory neurons under normal in vivo conditions (0.1–0.3 mM) (Richter et al. 1978). This is most likely caused by K^+ buffering by neighboring astrocytes and additional K^+ recycling mechanisms, such as activation of the Na^+/K^+-ATPases (D'Ambrosio et al. 2002). Therefore we expected the lack of Kir currents to impair K^+ uptake by astrocytes to affect the excitability of respiratory neurons located near by and to alter the rhythmic function of the entire network. We tested this hypothesis by quantifying network activity in rhythmic slices obtained from WT and Kir4.1$^{-/-}$ mice. The specific impairment of astroglial K^+ uptake in Kir4.1$^{-/-}$ mice was, however, not sufficient to significantly disturb respiratory network activity. This indicates that other mechanisms, probably involving activation of the Na^+/K^+-ATPases (D'Ambrosio et al. 2002), compensated for the loss of Kir4.1. This is consistent with previous slice experiments showing an arrest of respiratory network activity only in response to extracellular potassium levels exceeding 15 mM (Del Negro et al. 2001; Johnson et al. 2001).

Contribution of Kir4.1 channels to extracellular K^+ regulation in the developing respiratory network

D'Ambrosio et al. (2002) showed that Kir channels and Na^+/K^+-ATPases cooperate in the regulation of $[K^+]_o$. They found that K^+ released from hippocampal neurons was actively removed by both neuronal and glial Na^+/K^+-ATPase activity and by Kir channel mediated buffering (D'Ambrosio et al. 2002). According to their hypothesis, Na^+/K^+-ATPase activity persisted even when neuronal activity ceased and thereby caused an undershoot of $[K^+]_o$ under resting conditions (D'Ambrosio et al. 2002). This undershoot is normally balanced by K^+ extrusion through Kir channels. Our data support this putative mechanism, which also seems to be present in the respiratory network in the VRG. In Kir4.1$^{-/-}$ mice, astroglial K^+ fluxes were impaired; therefore astrocytes could not compensate for the pump-mediated undershoot of $[K^+]_o$ by extruding K^+ into the extracellular space. This is reflected in our data in which the undershoot in $[K^+]_o$ was greater in Kir4.1$^{-/-}$ mice than in WT mice (Fig. 6). Because application of Ba^{2+} further increased the $[K^+]_o$ undershoot, K^+ channels other than Kir4.1 may contribute to the maintenance of normal extracellular K^+ levels.

Different from what we initially concluded from our single-cell electrophysiological experiments, our extracellular K^+ measurements revealed that astroglial Kir channels, formed by the Kir4.1 subunit, only partially and very specifically contribute to $[K^+]_o$ regulation. In the developing VRG, Kir4.1 channels seem to fulfill two major tasks: they regulate baseline K^+ levels and compensate for the K^+ undershoot that occurs in response to neuronal activity and prolonged Na^+-K^+ pump activity. In our preparation, Kir4.1 channels were not significantly involved in the direct clearance of activity-dependent change in extracelllular K^+. Whether the function of Kir4.1 shifts later in maturation cannot be determined from our data because Kir4.1$^{-/-}$ mice die during the second postnatal week. New tools, such as a conditional knock-out of Kir4.1, are required to study the role of Kir4.1 in spatial buffering of potassium during intense neuronal activity in adult animals.

In conclusion, we confirmed that a particular glial Kir channel subunit (Kir4.1) is expressed in astrocytes in the ventral respiratory group. Astrocytes lacking Kir4.1 channels lost most of the inward driven K^+ currents, indicating that this channel is important for astroglial K^+ fluxes. Furthermore, Kir4.1 channels contribute to the regulation of baseline K^+ levels in the VRG. Finally, our data suggest that Kir4.1 channels shape extracellular K^+ levels by partially compensating for the undershoot in extracellular K^+ levels that accompanies neuronal activity.

ACKNOWLEDGMENTS

We thank J. C. Leiter for comments on the manuscript, A.-A. Grützner for excellent technical support, and P. G. Hirrlinger for instructive advice in mouse genotyping.

GRANTS

This work was supported by the Deutsche Forschungsgemeinschaft (DFG) through personal grants to C. Neusch (NE-767/3–1,3) and S. Hülsmann (SFB 406 TP C10) and through the DFG Research Center for Molecular Physiology of the Brain.

REFERENCES

Arcangeli A, Becchetti A, Mannini A, Mugnai G, De Filippi P, Tarone G, Del Bene MR, Barletta E, Wanke E, and Olivotto M. Integrin-mediated neurite outgrowth in neuroblastoma cells depends on the activation of potassium channels. *J Cell Biol* 122: 1131–1143, 1993.

Arcangeli A, Bianchi L, Becchetti A, Faravelli L, Coronnello M, Mini E, Olivotto M, and Wanke E. A novel inward-rectifying K^+ current with a cell-cycle dependence governs the resting potential of mammalian neuroblastoma cells. *J Physiol* 489: 455–471, 1995.

Ballanyi K. Protective role of neuronal KATP channels in brain hypoxia. *J Exp Biol* 207: 3201–3212, 2004.

Bredt DS, Wang TL, Cohen NA, Guggino WB, and Snyder SH. Cloning and expression of two brain-specific inwardly rectifying potassium channels. *Proc Natl Acad Sci USA* 92: 6753–6757, 1995.

Brockhaus J, Ballanyi K, Smith JC, and Richter DW. Microenvironment of respiratory neurons in the in vitro brainstem-spinal cord of neonatal rats. *J Physiol* 462: 421–445, 1993.

D'Ambrosio R, Gordon DS, and Winn HR. Differential role of KIR channel and Na(+)/K(+)-pump in the regulation of extracellular K(+) in rat hippocampus. *J Neurophysiol* 87: 87–102, 2002.

Del Negro CA, Johnson SM, Butera RJ, and Smith JC. Models of respiratory rhythm generation in the pre-Botzinger complex. III. Experimental tests of model predictions. *J Neurophysiol* 86: 59–74, 2001.

Gardner-Medwin AR, Coles JA, and Tsacopoulos M. Clearance of extracellular potassium: evidence for spatial buffering by glial cells in the retina of the drone. *Brain Res* 209: 452–457, 1981.

Gomeza J, Hülsmann S, Ohno K, Eulenburg V, Szöke K, Richter D, and Betz H. Inactivation of the glycine transporter 1 gene discloses vital role of glial glycine uptake in glycinergic inhibition. *Neuron* 40: 785–796, 2003.

Graβ D, Pawlowski PG, Hirrlinger J, Papadopoulos N, Richter DW, Kirchhoff F, and Hülsmann S. Diversity of functional astroglial properties in the respiratory network. *J Neurosci* 24: 1358–1365, 2004.

Haydon PG. GLIA: listening and talking to the synapse. *Nat Rev Neurosci* 2: 185–193, 2001.

Higashi K, Fujita A, Inanobe A, Tanemoto M, Doi K, Kubo T, and Kurachi Y. An inwardly rectifying K(+) channel, Kir4.1, expressed in astrocytes surrounds synapses and blood vessels in brain. *Am J Physiol Cell Physiol* 281: C922–C931, 2001.

Hülsmann S, Oku Y, Zhang W, and Richter DW. Metabolic coupling between glia and neurons is necessary for maintaining respiratory activity in transverse medullary slices of neonatal mouse. *Eur J Neurosci* 12: 856–862, 2000.

Jiang C, Xu H, Cui N, and Wu J. An alternative approach to the identification of respiratory central chemoreceptors in the brainstem. *Respir Physiol* 129: 141–157, 2001.

Johnson SM, Koshiya N, and Smith JC. Isolation of the kernel for respiratory rhythm generation in a novel preparation: the pre-Botzinger complex "island". *J Neurophysiol* 85: 1772–1776, 2001.

Kofuji P, Biedermann B, Siddharthan V, Raap M, Iandiev I, Milenkovic I, Thomzig A, Veh RW, Bringmann A, and Reichenbach A. Kir potassium channel subunit expression in retinal glial cells: implications for spatial potassium buffering. *Glia* 39: 292–303, 2002.

Kofuji P, Ceelen P, Zahs KR, Surbeck LW, Lester HA, and Newman EA. Genetic inactivation of an inwardly rectifying potassium channel (Kir4.1 subunit) in mice: phenotypic impact in retina. *J Neurosci* 20: 5733–5740, 2000.

Kusaka S, Horio Y, Fujita A, Matsushita K, Inanobe A, Gotow T, Uchiyama Y, Tano Y, and Kurachi Y. Expression and polarized distribution of an inwardly rectifying K^+ channel, Kir4.1, in rat retinal pigment epithelium. *J Physiol* 520: 373–381, 1999.

Lepple-Wienhues A, Berweck S, Bohmig M, Leo CP, Meyling B, Garbe C, and Wiederholt M. K^+ channels and the intracellular calcium signal in human melanoma cell proliferation. *J Membr Biol* 151: 149–157, 1996.

Li L, Head V, and Timpe LC. Identification of an inward rectifier potassium channel gene expressed in mouse cortical astrocytes. *Glia* 33: 57–71, 2001.

Magistretti PJ, Pellerin L, Rothman DL, and Shulman RG. Energy on demand. *Science* 283: 496–497, 1999.

Marcus DC, Wu T, Wangemann P, and Kofuji P. KCNJ10 (Kir4.1) potassium channel knockout abolishes endocochlear potential. *Am J Physiol Cell Physiol* 282: C403–C407, 2002.

Matthias K, Kirchhoff F, Seifert G, Huttmann K, Matyash M, Kettenmann H, and Steinhauser C. Segregated expression of AMPA-type glutamate receptors and glutamate transporters defines distinct astrocyte populations in the mouse hippocampus. *J Neurosci* 23: 1750–1758, 2003.

Müller M, and Somjen GG. Na(+) and K(+) concentrations, extra- and intracellular voltages, and the effect of TTX in hypoxic rat hippocampal slices. *J Neurophysiol* 83: 735–745, 2000.

Neusch C, Rozengurt N, Jacobs RE, Lester HA, and Kofuji P. Kir4.1 potassium channel subunit is crucial for oligodendrocyte development and in vivo myelination. *J Neurosci* 21: 5429–5438, 2001.

Newman EA. Regional specialization of the membrane of retinal glial cells and its importance to K^+ spatial buffering. *Ann NY Acad Sci* 481: 273–286, 1986.

Newman EA. Distribution of potassium conductance in mammalian Muller (glial) cells: a comparative study. *J Neurosci* 7: 2423–2432, 1987.

Newman EA. Inward-rectifying potassium channels in retinal glial (Muller) cells. *J Neurosci* 13: 3333–3345, 1993.

Newman EA, Frambach DA, and Odette LL. Control of extracellular potassium levels by retinal glial cell K^+ siphoning. *Science* 225: 1174–1175, 1984.

Nolte C, Matyash M, Pivneva T, Schipke CG, Ohlemeyer C, Hanisch UK, Kirchhoff F, and Kettenmann H. GFAP promoter-controlled EGFP-expressing transgenic mice: a tool to visualize astrocytes and astrogliosis in living brain tissue. *Glia* 33: 72–86, 2001.

Poopalasundaram S, Knott C, Shamotienko OG, Foran PG, Dolly JO, Ghiani CA, Gallo V, and Wilkin GP. Glial heterogeneity in expression of the inwardly rectifying K(+) channel, Kir4.1, in adult rat CNS. *Glia* 30: 362–372, 2000.

Ramirez JM, Quellmalz UJ, and Richter DW. Postnatal changes in the mammalian respiratory network as revealed by the transverse brainstem slice of mice. *J Physiol* 491: 799–812, 1996.

Ramirez JM, Schwarzacher SW, Pierrefiche O, Olivera BM, and Richter DW. Selective lesioning of the cat pre-Botzinger complex in vivo eliminates breathing but not gasping. *J Physiol* 507: 895–907, 1998.

Richter DW, Camerer H, and Sonnhof U. Changes in extracellular potassium during the spontaneous activity of medullary respiratory neurones. *Pfluegers* 376: 139–149, 1978.

Richter DW and Spyer KM. Studying rhythmogenesis of breathing: comparison of in vivo and in vitro models. *Trends Neurosci* 24: 464–472, 2001.

Rozengurt N, Lopez I, Chiu CS, Kofuji P, Lester HA, and Neusch C. Time course of inner ear degeneration and deafness in mice lacking the Kir4.1 potassium channel subunit. *Hear Res* 177: 71–80, 2003.

Smith JC, Ellenberger HH, Ballanyi K, Richter DW, and Feldman JL. Pre-Botzinger complex: a brainstem region that may generate respiratory rhythm in mammals. *Science* 254: 726–729, 1991.

Takumi T, Ishii T, Horio Y, Morishige K, Takahashi N, Yamada M, Yamashita T, Kiyama H, Sohmiya K, Nakanishi S, and Kurachi Y. A novel ATP-dependent inward rectifier potassium channel expressed predominantly in glial cells. *J Biol Chem* 270: 16339–16346, 1995.

Viemari JC, Burnet H, Bevengut M, and Hilaire G. Perinatal maturation of the mouse respiratory rhythm-generator: in vivo and in vitro studies. *Eur J Neurosci* 17: 1233–1244, 2003.

Wu J, Xu H, Shen W, and Jiang C. Expression and coexpression of CO2-sensitive Kir channels in brainstem neurons of rats. *J Membr Biol* 197: 179–191, 2004.